Design and characterization of carbon fiber-reinforced PEEK/PEI blends for Fused Filament Fabrication additive manufacturing

Audrey Diouf-Lewis[1], Rouhollah D. Farahani[1], Filippo Iervolino[1], Juliette Pierre[1], Yahya Abderrefaie[1], Martin Lévesque[1], Nicola Piccirelli[2], and Daniel Therriault[1*]

[1]*Laboratory for Multiscale Mechanics (LM²), Department of Mechanical Engineering, Polytechnique Montréal, Montréal, Canada*
[2]*Safran Composites, Itteville, France*
E-mail: daniel.therriault@polymtl.ca

Abstract

We formulated high temperature-resistant thermoplastic composite materials featuring high thermal and mechanical properties for the Fused Filament Fabrication (FFF) additive manufacturing process. The composite materials were blends of poly(ether ether ketone) (PEEK) and poly(ether imide) (PEI) with weight ratios of 100/0, 90/10, 80/20, 70/30, 60/40, 50/50 and 40/60 and all mixed using an extrusion process with 30 wt.% chopped carbon fibers (CFs). Differential Scanning Calorimetry measurements on the blends showed a significant increase of the single glass transition temperature, T_g, (up to 37°C for PEEK/PEI 40/60 formulation), when compared to the neat PEEK, indicating a good miscibility of PEEK and PEI. Microscopy observations using Scanning Electron Microscopy and X-ray microtomography revealed a good dispersion of CFs in the PEEK/PEI blend matrix and also the presence of some voids. Tensile mechanical testing results showed that the highest value of the Young's Modulus (13 GPa), among all the formulations, is obtained for the composition of reinforced PEEK/PEI (80/20) which also exhibited the lowest degree of porosity (2.90 %), and high printability in the FFF process (i.e., high visual quality of the printed parts with no major printing issues). The materials developed here will help move towards manufacturing of functional prototypes made of high-performance composites (e.g., high mechanical properties and high service temperature) using FFF additive manufacturing process for various aerospace applications.

Keywords: Additive manufacturing, Thermoplastic blends, Carbon fiber, PEEK, PEI

1. Introduction

Additive manufacturing (AM), or 3D printing, can deliver complex shapes with an expanding range of printable materials [1–3]. As one of the most popular 3D printing technologies, Fused Filament Fabrication (FFF), also known as Fused Deposition Modeling (FDM), is an inexpensive and easy-to-use technique that is based on the layer-by-layer deposition of partially melted thermoplastic-based filaments. The FFF technique uses, as its printing materials, various thermoplastics ranging from polylactic acid (PLA) to engineering thermoplastics (e.g., nylon) and their reinforced composites. However, these materials are only suitable for low temperature applications (i.e., <45°C), which excludes their use in advanced engineering applications such as aerospace where temperatures >120°C are encountered. Consequently, the choice of printable materials has to be expanded to high-performance thermoplastics such as poly(ether ether ketone) (PEEK) and poly(ether imide) (PEI). PEEK is a semi-crystalline polymer and PEI is an amorphous polymer with glass transition temperatures (T_g) of 147°C [4] and 217°C [5], respectively. Due to their excellent chemical, mechanical, and thermal properties, PEEK and PEI are among the most interesting materials in aerospace industry and with high potential to replace numerous heavy metallic parts offering cost and environmental benefits [6,7]. However, the adaption of these high-performance polymers to additive manufacturing is particularly challenging mainly due to their high melt viscosities and high processing temperatures. 3D printing of these materials requires special printing conditions such as high printing temperatures (e.g., nozzle extrusion temperature beyond 340°C) and temperature-controlled printing environment (e.g., ambient temperature close to their T_g). The FFF printing at high temperatures in addition to a hard control of the printing

environment's temperature may cause several common issues such as delamination and warping [8]. In the case of semi-crystalline polymers like PEEK, FFF at high temperatures affects the degree of crystallinity and creates different crystalline regions in the same 3D printed part, directly affecting the mechanical properties [9–11]. A proper FFF printing condition can also enhance inter-layer adhesion [8,10,12], which is a very important parameter to obtain high-quality 3D printing parts.

Most neat thermoplastics including PEEK and PEI cannot reach the stiffness and/or temperature requirements for aerospace applications (e.g., 2.6×10^6 m^2s^{-2} for the specific stiffness of polyether ether ketone (PEEK), when compared to 26×10^6 m^2s^{-2} for aluminum). Reinforcing thermoplastics with fillers such as carbon fibers (CF) [13–18], carbon nanotubes [18–22] and graphene [23] is an effective approach to significantly improve their mechanical and thermal performance. Particularly for CF-reinforced PEEK composites, it has been reported that the tensile strength and stiffness increase as function of the fillers concentration, without significantly changing the T_g or the crystallinity [15,17,24]. An increase of 8°C of the T_g of PEI polymers was also observed after the addition of carbon fibers [21]. However, the incorporation of CFs into polymers, even at low concentrations (e.g., 5 wt.%) of CFs is reported to create porosity in the resulting composites [25]. Porosity or voids in fiber-reinforced polymer composites are suspected to adversely affect their mechanical properties [26].

Blending two or more polymers is another approach that can help combine their properties and possibly have a synergetic effect [27]. PEEK possesses excellent mechanical properties but a relatively low softening temperature (T_g: ~143°C). PEI possesses lower mechanical properties but a significantly higher T_g (~217°C). Thanks to their high miscibility [28–32], blending PEEK and PEI enables tailoring the blend desired properties including, but not limited to, chemical resistance

[30], toughness [30], thermal behavior (e.g., T_g, T_m) [28,32,33], and mechanical properties [27]. Several recent works studied the FFF 3D printing of CF-reinforced materials with a single matrix of PEEK [34–36] and single matrix of PEI [37,38]. To the best of authors' knowledge, no works have reported the processing and utilization of PEEK and PEI blends reinforced with CFs for the FFF 3D printing. Designing PEEK/PEI blends and their reinforced composites and adapting them for AM is expected to have strong potential for the printing of functional prototypes for the more demanding aerospace applications.

The aim of this work is to develop high-performance thermoplastic composite materials, composed of PEEK, PEI and chopped CFs, featuring high mechanical and thermal properties while exhibiting high printability for the FFF additive manufacturing process. The new materials developed for 3D printing were formulated to meet some specific material requirements for aerospace applications (e.g., high temperature service, high mechanical performance), since commercially available printing filaments only partially meet the needs. The formulation of PEEK and PEI blends reinforced with CFs, called hereafter CF-PEEK/PEI blend, involved finding the best composition with an optimal thermal and mechanical properties while achieving high quality prints. Blends of PEEK and PEI with various weight ratios were loaded with 30 wt.% CFs and were characterized for their mechanical (i.e., tensile testing of filaments), thermal (i.e., using differential scanning calorimetry (DSC)) and microstructure properties as well as their printability in FFF AM. Scanning electron microscopy (SEM) and X-ray microtomography (μ-CT) were used to better understand the relation of materials microstructure (e.g., CF-matrix adhesion, CFs' orientation and porosity content) and their mechanical properties. Finally, as an indication of materials printability, some demonstrators with complex shapes were successfully printed using the selected CF-PEEK/PEI blend compositions.

2. Material and methods

2.1. Materials

The high temperature-resistant thermoplastics (HTRTs) used in this study were PEEK pellets (grade 90G manufactured by Victrex, USA) and PEI pellets (ULTEM 1010 from Sabic, supplied by Nexeo Solutions 3M, Canada). Chopped carbon fibers (type 83) purchased from Zoltek Corporation (USA) have a nominal length of 6 mm, 1.5 wt.% of a sizing agent, a tensile modulus of 242 GPa and a tensile strength of 4137 MPa, according to the manufacturer [39].

2.2. Blending process

The device used for the melt mixing was a twin-screw micro-extruder (DSM Xplore, 5 cc micro-compounder, Netherlands). Before the mixing, chopped CFs, PEEK and PEI were dried overnight in an oven at 150°C. The PEEK and PEI pellets were first incorporated into the micro-extruder at a constant temperature of 370°C with a screw rotating speed of 50 RPM for 2 min. By keeping the same temperature and rotating speed, the chopped CFs with a proportion of 30 wt.% of the total mixture were then fed into the micro-extruder to be mixed with the melted polymers. After the feeding step, the screw rotating speed was increased to 100 RPM for 5 min of mixing using the recirculating mode. With the micro-extruder die having a diameter of 2 mm, the obtained filament, called hereafter the extruded filament, had a diameter ~1.75 mm. While keeping CF's weight fraction constant at 30 wt.% in all mixtures, different concentrations of PEEK/PEI blends were processed with weight ratios of 100/0, 90/10, 80/20, 70/30, 60/40, 50/50 and 40/60. Hereafter, the CF-PEEK/PEI compositions are named by their weight ratio of PEEK/PEI. For example, CF-PEEK/PEI 90/10 for the composition of, 90 wt.% PEEK and 10 wt.% PEI while CFs loading is constant at 30wt.%. Unreinforced blends were also prepared for comparison purposes.

2.3. Thermal properties characterization

Differential scanning calorimetry was carried out by using a TA instrument DSC Q1000, USA. A sample of 5 mg from extruded filament was placed in an aluminum pan, and then submitted to a heat-cool-heat DSC measurement. The principle of a heat-cool-heat measurement is to erase the thermal history of the material. The heating and cooling runs were conducted from 50°C to 390°C using a constant rate of 10°C/min. During the measurement, a purge of nitrogen with a flow of 50 mL/min was applied. Different transitions were recorded: the cold crystallization temperature (T_{cc}) on the first heating run; the T_g and the melting temperature (T_m) were taken on the second heating run; the crystallization temperature (T_c), and the degree of crystallinity ($X_c\%$) were obtained from the cooling run. The T_g was also determined with higher precision using modulated DSC (mDSC) measurement [40]. A modulated heating cycle was applied to measure the reversible and non-reversible transitions. The temperature program operated from 100°C to 200°C, with a rate of 2°C/min, for a period of 60 s, and a modulation amplitude of 1.27°C, on a 15 mg sample.

2.4. Tensile mechanical characterization

2.4.1 Sample preparation

The tensile mechanical characterization was performed on filaments, hereafter referred as FFF filaments. The FFF filaments with a diameter of ~0.6 mm were fabricated by further extruding the filament obtained after the mixing process (i.e., the extruded filaments, see Section 2.2) using an FFF 3D printer (AON3D-M2, Canada). The hot end temperature and printing speed were 400°C and 5 mm/s, respectively. The FFF filaments were cut into specimens of 15 cm length for tensile mechanical testing. Before the test, at least 5 specimens for each CF-PEEK/PEI composition were dried at 150°C for 15 h under vacuum.

2.4.2 Tensile test

The tensile tests were conducted using an MTS Insight electromechanical testing device, equipped with a 100 N load cell running under MTS Testforce software. According to ASTM D3822 standard [41], the grip velocity was set at 10 mm/s. The test was carried out with a virtual extensometer measured by a Direct Image Correlation (DIC) system, composed of two high speed cameras taking pictures every 250 ms during the test. The virtual extensometer was placed on the grip behind the specimen to allow the detection of the displacement by using VIC3D software from Correlated Solutions.

2.5. Microstructural characterization

Scanning electron microscopy (SEM) was used to characterize materials microstructure observed on the fractured surface of the filaments. Before the SEM observation, the filament specimens were fractured using nitrogen and sputtered with gold at 30 mA for 20 s. The SEM machine used was a JEOL JSM7600F (USA), equipped with a lower second electron image (LEI) detector. The operating condition of acceleration voltage was 2kV. X-ray microtomography (μ-CT) was used to characterize the CF-PEEK/PEI filament microstructures in three dimensions and to observe the CFs orientation and the presence of voids. μ-CT was performed with an Xradia 520 Versa device from Zeiss, Canada. FFF filaments were analyzed at an acceleration voltage of 50 kV, a power of 4 W, an objective of 10 ×, and an exposure time of 10 s per scan. Images for this paper were generated using Dragonfly Software from Object Research Systems ORS inc, Canada.

2.6. Large production of filaments for FFF 3D printing

Section 2.2 to Section 2.5 discussed the experimental details for the materials selection phase. As the micro-extruder with a relatively low volume capacity of 5CC was used to mix the materials for

that phase, a semi-industrial co-rotating twin-screw extruder (Bühler 20 mm, Bühler Canada, Canada) with an *L:D* ratio of 40 was employed for the fabrication of larger quantity of materials (1 kg spooled filaments) for FFF 3D printing of a few demonstrators. Formulations with the most promising mechanical and thermal properties were manufactured into spooled filaments of ~1.75 mm in diameter. The goal was to further investigate the printability of CF-PEEK/PEI blends in the FFF 3D printer and the quality of the printed demonstrators. The filament making process was carried out in two stages, mixing and spooling. CFs and polymers were dried overnight at 150°C, and then mixed using the twin-screw extruder at 150 RPM with an output of 2 kg/h. After the mixing, the extruded filaments were cut into pellets at the end the extrusion line. Pellets were then dried at 150°C for 4h and processed to filaments using a Brabender single-screw extruder with a screw length L:D of 25D (Brabender® GmbH & Co. KG, Duisburg, Germany) and a filament spooler (Filabot, USA). The screw rotation speed and the extrusion temperature were set at 20 RPM and 400°C, respectively. The diameter of the extruded filaments was continuously monitored for their uniform ovalities using a Zumbach system (Zumbach ODAC 18XY unit and Zumbach USYS unit) from Zumbach Electronics Corporation, Mount Kisco, NY, USA. The steadiness of the diameters was achieved by a continuous control of the pulling rate and the flow rate. Finally, the spools were dried for 4 h at 150°C and stored in plastic bags under vacuum.

2.7. Printability and 3D printing quality evaluation

Prior to FFF 3D printing of the demonstrators, each spool was dried in the oven under vacuum at the temperature of 150°C for at least 4 h. The FFF 3D printing was carried out using the AON3D-M2 3D printer with a temperature-controlled enclosure set at 120°C and using a slicing software (Simplify3D, USA). The specific printing parameters used for each 3D printed demonstrators will

be discussed in Section 3 (Results and discussion). The print quality was assessed under optical microscopy using an Olympus SZX-12 stereomicroscope. A surface roughness measuring device (Mitutoyo FORMTRACER SV-C4000, USA) was used to evaluate the surface roughness of 3D printed structures. With the automatic compensation of radius and inclination, the roughness profile was measured at an evaluation length λ of 4 mm and a cutoff of 0.8 mm. The roughness test was repeated at least 5 times. The surface roughness was evaluated with the arithmetical mean roughness (*Ra*), which is the most commonly used profile roughness parameter. On a profile roughness curve, *Ra* is defined as the arithmetic average value identified from the deviations about the center line within the evaluation length.

3. Results and discussion

3.1. Thermal behavior of CF-PEEK/PEI composite materials

DSC tests were carried out to investigate the thermal transitions of the PEEK/PEI blend reinforced with CFs and also to assess the PEEK/PEI miscibility. **Fig. 1** compares the DSC curves of CF-PEEK/PEI blends of different compositions as a function of the temperature and the heat flow for the second heating run (**Fig. 1a**) and the cooling run (**Fig. 1b**). On the second heating run, an endothermic peak is observed for each composition at a temperature ranging between 337.0°C and 344.8°C. This peak corresponds to the melting transition temperature of the semi-crystalline materials like PEEK and becomes broader as the PEI content increases in the blend. For comparison purposes, the composition CF-PEEK/PEI 0/100, which is the formulation without PEEK, is also shown and it has no melting transition temperature peak because PEI is an amorphous polymer. The thermal transition peak observed for the CF-PEEK/PEI 0/100 at 217.1°C is attributed to the T_g of the PEI. In **Fig. 1b**, exothermic peaks are observed at the temperature

range of 262.3°C to 307.8°C and correspond to the crystallization temperature for the different CF-PEEK/PEI compositions. As previously observed for the T_m, the crystallization peak becomes larger with the increase of the PEI content in the blend. The observed shifts in the crystalline and melting peaks with the increase of PEI content might likely be due to the amorphous state of PEI which likely affected the blends' crystallization [42]. All the studied CF-PEEK/PEI formulations follow the semi-crystalline behavior of PEEK, by showing a single peak for their melting and crystalline temperature transitions. In addition, the shifting of these two temperature transition peaks as a function of PEEK/PEI content can be attributable to the miscibility of PEEK and PEI in the CF-PEEK/PEI blends.

Table 1 reports the DSC temperature values of T_c and T_m of the CF-PEEK/PEI blends extracted from the cooling run and the second heating run, respectively. A considerable decrease of melting temperature (~8°C) of the blends with the increase of the PEI content is observed that is possibly due to interlamellar segregation of the PEI chains [28]. The resulting degree of crystallinity X_c% of CF-PEEK/PEI blends is also reported in **Table 1**. The degree of crystallinity was determined from the melting peaks in **Fig. 1a**, by dividing the measured enthalpy of fusion of the sample by the enthalpy of fusion of the 100% crystalline PEEK, 130 J/g [4], and also by considering the weight fraction of PEEK [28]. The addition of PEI into the PEEK increased the degree of crystallinity for all the blends. The crystallinity of the blends shows a trend of first increasing with the increase of PEI proportion from 31.9% for the CF-PEEK/PEI 100/0 formulation to a value of 40.5% for the CF-PEEK/PEI 80/20 formulation. This increase might be attributable to the PEI content at which the PEI contributed advantageously to the rearrangement of the PEEK chains by increasing the blends interlamination fluidity [30]. For the CF-PEEK/PEI blends with PEI content above 20 wt.%, the X_c% first decreased to 37.7% for the CF-PEEK/PEI 70/30 formulation and

then increased to 41.0% for the CF-PEEK/PEI 50/50 formulation. It has been reported in the literature that three modes of crystal organization are possible during the crystallization of miscible PEEK/PEI blend in the amorphous state [43,44]. PEI can be completely rejected from the growing crystal, be trapped between lamellar crystal structures, or rejected between individual lamellar. The relative rate of PEEK crystal growth and PEI diffusion could result in any of the three modes to occur. The increase of PEI content lowers the overall viscosity of the blend in a favorite of higher rate of PEI diffusion and may results in a faster crystallization. All these factors and their impacts may justify our results for the degree of crystallinity.

The T_g of CF-PEEK/PEI blends was determined using modulated DSC (mDSC) experiments because it was not detectable in the second heating run curves. T_g values are compared with the Fox T_g. Fox T_g is calculated from the Fox equation, **Equation 1**, which approximates the T_g expected from a miscible blend [45]:

$$\frac{1}{T_{gFox}} = \frac{w_1}{T_{g1}} + \frac{w_2}{T_{g2}} , \quad (1)$$

where w_1 and w_2 are the weight fractions of the blend constituents and T_{g1} and T_{g2} are their respective T_g. The measured T_g and predicted T_{gFox} are reported in **Table 2.** The measured T_g of the different compositions fit very closely (up to 4°C difference) with T_{gFox} approximation and both increase with the increase of the PEI content. These results further suggest that our CF-PEEK/PEI blends are fully miscible [28,29,31]. However, as summarized in **Table 2**, CF-PEEK/PEI compositions 70/30, 60/40, 50/50, and 40/60 exhibit a very weak peak for second T_g at the average temperature of 212.3 ± 3.5°C. This second T_g might possibly be attributed to some non-miscible part in these blends. As observed in the literature for neat PEEK/PEI blends, two T_g can be detected: one attributed to the glass transition which takes place in the amorphous state and

the second one to the glass transition occurring in the semi-crystalline state [46]. During the crystallization of the PEEK in the blends, if phase segregation occurs, a semi-crystalline state of the blend is created [46]. Based on the values obtained for the second T_g, it seems that the PEI-dominant amorphous phases are formed at PEI contents at 30 wt.% and higher. Based on the DSC results, it can be concluded that PEI advantageously influences the crystallization of CF-PEEK/PEI blends while improving their T_g (up to 37°C in this study).

3.2 Mechanical properties characterization

As schematically shown in **Fig. 2a,** tensile mechanical tests were conducted on the FFF filaments to compare the Young's modulus of the various CF-PEEK/PEI blends. The corresponding unreinforced blends were also prepared and tested to study the reinforcing effect of CFs. **Fig. 2b** shows representative stress-strain curves of typical neat PEEK, when compared to the 30 wt.% reinforced PEEK (i.e., CF-PEEK/PEI 100/0). At least five specimens were tested for each formulation and the errors fall within 3% of the standard deviations. The elastic domain is much steeper for the CF-PEEK/PEI 100/0 blend than for the neat PEEK. In addition, both neat PEEK and the CF-PEEK/PEI 100/0 exhibit the stress peaks at 91 MPa and 101 MPa, respectively. The strength detected for CF-PEEK/PEI 100/0 indicates that it is more brittle than neat PEEK. **Fig. 2c** shows the Young's modulus of different PEEK/PEI blend compositions for both unreinforced and reinforced blends. For the unreinforced blends, the values of Young's modulus were ranging between 2.7 and 3.6 GPa. The addition of 30 wt.% CFs increased the Young's modulus ranging from 261% to 350%. For CF-PEEK/PEI blends, the average Young's modulus varies between 13.0 GPa and 10.1 GPa, decreasing with the increase of PEI content in the PEEK/PEI blend with the exception of CF-PEEK/PEI 80/20 and 60/40 formulations. CF-PEEK/PEI 100/0 and CF-

PEEK/PEI 80/20 exhibit the highest modulus of 13.0 GPa. Our results are comparable to or exceeding the best reported in the literature for short carbon fibers-reinforced PEEK materials [15,23,47]. Several factors, including the degree of crystallinity, the void content and their size, the PEEK/PEI proportions, and the microstructure of the blends that could be different from one to another, contributed to the measured value of the Young's modulus for each blend. The degree of crystallinity is assumed to have a direct impact on the mechanical properties of the blend and might justify the different behavior of CF-PEEK/PEI 80/20 and CF-PEEK/PEI 60/40 formulations [27]. As observed with the DSC results, CF-PEEK/PEI 80/20 formulation showed a high degree of crystallinity (i.e., 40.5%) that justifies the highest value of the modulus (equals to CF-PEEK/PEI 100/0) among other compositions.

3.3 Microstructural characterization

3.3.1. SEM observation of extruded filaments

The extruded filaments' fractured surface was observed under SEM to investigate the CFs dispersion and their adhesion to PEEK/PEI matrix. **Fig. 3** shows the SEM images at different magnification of four representative filament compositions: (a) neat PEEK, (b) CF-PEEK/PEI 100/0: the formulation without PEI, (c) CF-PEEK/PEI 80/20: the formulation with the highest degree of crystallinity, and d) CF-PEEK/PEI 50/50: the composition with the same ratio of PEEK and PEI. The SEM image of fractured surface of neat PEEK, in **Fig. 3a**, shows a typical smooth surface of the polymeric material. In **Fig. 3b-d**, the SEM images of the fractured surfaces are rougher with the presence of CFs distributed all over the surface areas, and the presence of voids with diameters up to 50 µm. A good distribution of CFs throughout the extruded filament is observed for all the reinforced compositions, confirming the effectiveness of our mixing process

in the micro-extruder and possibly the effect of shearing in the printing head. From the images magnified at ×2000 in **Fig. 3b-d**, it is observed that carbon fibers are mainly wrapped by the polymeric matrix, which suggests adhesion between the CF and PEEK/PEI, although some CFs pull-out is also observed. The CFs sizing materials possibly contributed to fiber-matrix adhesion. Although the CFs used in this work feature a sizing recommended for high temperature mixing with PEEK and PEI polymers, there might still be the possibility of some decomposition of the sizing at high processing temperatures. In addition, the shrinkage of PEEK materials may have also contributed to an imperfect fiber-matrix adhesion. However, these are hypotheses and are not experimentally verified in our work.

3.3.2. μ-CT observation of FFF filaments

Fig. 4 shows μ-CT images taken during the observation of FFF filaments. **Fig. 4a** represents the 3D reconstruction of the μ-CT images for the cylindrical-shape FFF filament. We identified the cylinder's height as the *z* axis which corresponds to the direction of the extrusion through the nozzle, and the *xy* plane as the cylinder surface or a slice section. The *zx* plane is a cross section through the height direction. **Fig. 4b-e** show the μ-CT images of the *xy* and *zx* planes of neat PEEK, CF-PEEK/PEI 100/0, CF-PEEK/PEI 80/20, and CF-PEEK/PEI 50/50 FFF filaments, respectively. On the *xy* plane, the presence of round shapes and white dots distributed throughout each sample are observed only in the reinforced FFF filament compositions. The white dots with a diameter of 7 μm observed in the *xy* plane, corresponding to white lines in the *zx* plane, are attributed to carbon fibers. The round shapes are believed to be voids that were also observed in the SEM images of the extruded filaments. No voids are seen in the image of the neat PEEK, suggesting that the addition of CFs is mainly responsible for the creation of voids in the reinforced blends. In addition,

CFs and voids were segmented and their 3D visualization, for the case of CF-PEEK/PEI 80/20, is shown in **Video 1 in Supplementary Information.** The scanned sample is an FFF filament with a diameter of 0.6 mm, extruded through a nozzle at 400°C with a speed of 5 mm/s. Segmentation allows us to distinguish the voids from the CFs and the matrix, to facilitate their visualization and obtain further analytical information like the voids size-distribution and CF length and orientation. **Fig. 5a-c** show the μ-CT analysis by image segmentation of the voids of CF-PEEK/PEI 100/0, CF-PEEK/PEI 80/20 and CF-PEEK/PEI 50/50, respectively. In **Fig. 5a(i)** and **5a(ii)**, the 3D visualization of the CF-PEEK/PEI 100/0 filament shows that the voids are dispersed throughout the filament with smaller voids close to the external surface of the filament while bigger ones in the filament's center. The figure shows that the voids diameters range from 1 to 28 μm. A similar dispersion state is observed for CF-PEEK/PEI 80/20 in **Fig. 5 b(i)**, and the voids diameter is measured from 1 to 25 μm as shown in **Fig. 5b(ii**). In the case of CF-PEEK/PEI 50/50, in **Fig. 5c(i)**, relatively large size voids are observed. According to their related color range in the graph presented in **Fig. 5c(ii)**, most of the voids size diameter are ranging from 30 to 50 μm. The 3D visualization analysis obtained by three segmentation trials also revealed that the degree of porosity of the CF-PEEK/PEI 100/0, CF-PEEK/PEI 80/20 and CF-PEEK/PEI 50/50 were determined at ~3.90%, ~2.40% and ~19.70%, respectively. The high degree of porosity for CF-PEEK/PEI 50/50 formulation might be attributable to the viscosity and microstructure of the blend. Higher PEI loading decreases the overall melt viscosity of the composites, possibly letting the trapped gas (e.g., air bubbles) to expand and also leading to partially independent movement of the CFs and PEEK/PEI matrix during extrusion [48]. The high amount of PEI in the CF-PEEK/PEI 50/50 formulation might have increased the affinity of the CFs to move to amorphous and less viscous PEI phase. Finally, PEI has higher moisture absorption than PEEK and it might be more

problematic at a higher PEI loading, resulting in the trapped bubbles during the extrusion process. Further study will be required to systematically quantify the sources for the creation of the voids in our PEEK/PEI blends. The high degree of porosity and the larger void size in CF-PEEK/PEI 50/50 likely contributed to its lower Young's modulus compared to the other two formulations.

Fig. 6a(i), 6b(i), and 6c(i) represent the segmentation analysis of CFs on the μ-CT images of the same three representative CF-PEEK/PEI blends, in a 2D view in the *xy* axis, and in a 3D visualization of the CF after segmentation. The segmentation assigned a color to each CF as function of its length. It is observed that carbon fibers are mostly oriented along the *z* axis, which corresponds to the direction of extrusion through the 3D printing nozzle. **Fig. 6a(ii), 6b(ii), and 6c(ii)**, shows the graph of the CF segmentation of the three CF-PEEK/PEI blends. In the case of CF-PEEK/PEI 100/0, according to the CF segmentation color, the related graph indicates that the majority of CFs length (in yellow) is above 890 μm. For CF-PEEK/PEI 80/20 and CF-PEEK/PEI 50/50, the majority of the CFs reach the length of 820 and 760 μm, respectively. Smaller size CFs (purple and blue) in all these three CF-PEEK/PEI blends are attributed to the fibers that were originally shorter or broken during the mixing process or to the fibers whose actual length is not entirely within the analysis area. The volume fraction of CFs in the CF-PEEK/PEI 100/0, CF-PEEK/PEI 80/20 and CF-PEEK/PEI 50/50 were determined at 23.6, 19.7 and 21.6 %, respectively.

3.4 FFF printability of CF-PEEK/PEI blends

The printability of the two most promising CF-PEEK/PEI blends, i.e., showing the best results in terms of mechanical and thermal properties, and void content, is investigated and compared to that of the neat PEEK. **Fig. 7a-c(i,ii)** show the optical images of vase and cubohemioctahedron shapes 3D printed with the three materials of neat PEEK, CF-PEEK/PEI 100/0 and CF-PEEK/PEI 80/20.

Table 3 lists the printing parameters used for the 3D printing of the parts. The vase structures were fabricated to assess the ability of the three representative formulations to be printed in a continuous mode (vase mode), that consists in the 3D printing of a structure with a single filament. The cubohemioctahedron shapes are representative of the 3D printing in a default (normal) mode. For all the three materials, the expected shapes were achieved, and the prints seem to be of acceptable visual quality, demonstrating their high printability in a continuous and default modes. However, significant cracking and warping were observed for the parts printed using the neat PEEK, possibly occurred during the post-printing (i.e., cooling phase). To further investigate the warping issue, rectangular specimens were 3D printed as shown in a side view in **Fig. 7a-c(iii)**. In the case of the neat PEEK, a structure lifting, varying by 13.5 ± 4.5 mm on average, is observed. This type of the printing issue was observable during the three printing attempts. The lift indicates that the material started to warp at its extremities during 3D printing, almost in the middle of printing and became worse towards the end. In the case of the reinforced blends, i.e., CF-PEEK/PEI 100/0 and CF-PEEK/PEI 80/20, no important warping was observed that could be due to the presence of CFs as they add dimensional stability to the polymer matrix by increasing thermal conductivity and decreasing coefficient of thermal expansion (CTE) [49].

Fig. 8a-c compare the printing quality of three rectangular cuboid structure in a (i) macroscopic and (ii, iii) microscopic views. A major defect in **Fig. 8a(i)** is observed for the neat PEEK on the side face which might be related to a layer-layer separation. The layer separation or delamination takes place once the bonds between successively printed layers are weak. According to the literature, this type of defect is a common issue for 3D printed PEEK materials due to the printing at high temperatures and difficulty in controlling of the cooling conditions [12]. For the blends, however, the surfaces of their cuboid seem smooth with no large defects as it can be seen in **Fig.**

8b(i) and **8c(i)**. **Fig. 8a-c(ii)** show the optical microscopic images of the *zy* plane of each rectangular cuboid **and 8a-c(iii)** compare the *xy* top surface of the rectangular cuboid, made of neat PEEK, CF-PEEK/PEI 100/0 and CF-PEEK/PEI 80/20, respectively. For the neat PEEK, in the *zy* face, a good adhesion between the layers is seen, however, a repetitive delamination is created in the center of the printed specimen. Regarding the *xy* top surface, no clear distinction of the deposited FFF filament is observed and a good adhesion between the FFF filaments and the outline perimeter is noticed, both indicating a very good inter-filament adhesion. For the CF-PEEK/PEI 100/0 and CF-PEEK/PEI 80/20, the optical microscopic images of the *zy* face show homogenous and continuous staking of the layers. For the first bottom layer of CF-PEEK/PEI 100/0, a slight separation from the other layers is also observed, which might probably be due to the part removing from the 3D printer building bed. Regarding the *xy* top layer particularly for CF-PEEK/PEI 100/0, the distinction of two consecutive FFF filaments can be observed (highlighted with red arrows). As consecutive filaments are not merged, their inter-filament bonding seem weaker than the one made of the neat PEEK. Concerning CF-PEEK/PEI 80/20, the inter-filament space is smaller and merged at some parts. However, for both reinforced blends, the overlap with the outline perimeter is well realized, as no gaps between the outline filament and the infill filament are observed.

In **Fig. 9a-c,** the surface roughness of the rectangular cuboid's top layer of the neat PEEK, CF-PEEK/PEI 100/0 and CF-PEEK/PEI 80/20 is compared, according to **(i)** the lengthwise direction, and **(ii)** the crosswise direction, respectively. The corresponding analyzed surfaces are also shown using the microscopic images in **(iii)**. The roughness curves present the profile height as a function of the analyzed length, and the central line is identified at the height of 0 µm. In **Table 4**, the arithmetical mean roughness parameter *Ra* are reported according to the lengthwise and the

crosswise directions. The three representative materials show very different roughness profiles in the lengthwise direction, as shown in **Fig. 9a-c(i)**. A straight line with small fluctuations and very close to the central line is observed for the neat PEEK, indicating that the surface is smooth in the lengthwise direction. For the CF-PEEK/PEI 100/0 and CF-PEEK/PEI 80/20, the roughness profiles show significant irregularities with the highest amplitude for CF-PEEK/PEI 100/0. The roughness profile of the reinforced blends indicate that the surface has printing defects. For instance, for CF-PEEK/PEI 100/0 (**Fig. 9b(iii))**, some inter-filament gaps (shown by red arrows) are present between two consecutive FFF filaments, and defects (shown by red circle) are also observed in the middle of some FFF filaments. In the case of CF-PEEK/PEI 80/20, the amplitude of irregularities is less significant and in a good agreement with the microscopy images in **Fig. 9c(iii)**. The lowest value of *Ra* was measured for the neat PEEK at 0.2 µm corresponding to the smoothest surface. The *Ra* values for CF-PEEK/PEI 80/20 and CF-PEEK/PEI 100/0 were 3.2 µm and 8.5 µm, respectively.

Fig. 9a-c(ii) compares the roughness profiles in the crosswise direction. The irregularities amplitude of the neat PEEK is the highest with a frequency of 1200 µm in length. The repetition consists in two peaks: the one at the height of 150 µm and the second at the average height of 30 µm. These two peaks that repeat corresponds to the top of two consecutive FFF filaments for which the amplitude coincides with the printing direction through the nozzle along the lengthwise direction. In the case of the reinforced blends, i.e., CF-PEEK/PEI 100/0 and CF-PEEK/PEI 80/20, the roughness profile for the crosswise direction showed that both curves of roughness profile are composed of many peaks and irregularities. The roughness irregularities are, however, less significant than for the case of the neat PEEK. With *Ra* value of 6.6 µm, the smoothest material in the crosswise direction is CF-PEEK/PEI 80/20, followed by 14.6 µm for CF-PEEK/PEI 100/0 and

37.9 µm for the neat PEEK. Among these three materials, the CF-PEEK/PEI 80/20 formulation exhibits least amount of variation in height amplitude in both lengthwise and crosswise directions. In line with the obtained results for the mechanical properties, the CF-PEEK/PEI 80/20 formulation seems the most promising material as it also combines a visually good inter-filament bond with the least surface roughness value. Therefore, this formulation was further assessed for its printability for 3D printing of high-quality complex parts.

Fig. 10 illustrates a few representative structures used as demonstrators that were successfully printed with CF-PEEK/PEI 80/20. The printing parameters for those structures are listed in **Table 5**. The PolyPearl tower showed in **Fig. 10a,** is a 3D printing model that includes several difficult-to-print elements such as 45° overhang, roundness, smooth curved surfaces, fine bridging, fine details, etc. The three supporting legs of the PolyPearl Tower were printed at 45° which is referred as the critical angle that an FFF 3D printer can handle before using additional support. On both ball sections of the tower, there is an overhang section that is well formed, flat and circular, and the roundness is well performed. In addition, smooth curved (ii) and fine bridging (ii) are well achieved, and fine details are present (iii). **Fig. 10b** presents a simplified version of a honeycomb sandwich structure consisting of three layers: a low-density core sandwiched between two skin-layers. This type of structures is very popular in aircraft, automotive and transportation fields. In our sandwich structure, the top skin layer was partially printed just for a better visualization of the honeycomb core geometry. **Fig. 10c**, is a picture of a 3D printed ring connected to an oil ruler commonly used to check vehicle's oil level. The use of CF-PEEK/PEI 80/20 blend for this automotive application is appropriate because this material is able to withstand the high temperatures generated by an engine and also be chemical resistant. **Fig. 10d** presents an articulated octopus printed continuously, showing the ability of CF-PEEK/PEI 80/20 to be printed

in complex shapes. Indeed, articulated 3D printed structures are increasingly being used for complex biological researches [50]. The high quality of the complex structures showed in **Fig. 10** further proves the printability and viability of CF-PEEK/PEI 80/20 as a novel FFF 3D printing material featuring several interesting properties.

4. Conclusion

This paper reports the investigation of carbon fiber-reinforced PEEK/PEI blends featuring high mechanical and thermal properties while maintaining a high printability for the FFF 3D printing process. The PEEK and PEI were shown to be miscible in the developed formulations with the PEI content below 30 wt.%. According to the microstructural characterization, CFs were well dispersed within the PEEK/PEI blends and also revealed a good adhesion with the blend matrix. The tensile test showed that the addition of CFs induced a significant improvement of the Young's modulus up to 350% when compared to the unreinforced materials. The presence of voids was also detected in all CF-PEEK/PEI formulations. The tensile and μ-CT analyses indicated that voids can adversely contribute to the mechanical properties. The CF-PEEK/PEI 100/0 and CF-PEEK/PEI 80/20 were the two most promising formulations by exhibiting the highest Young's modulus of 13 GPa and the lowest degree of porosity of 3.90% and 2.40 %, respectively. Also, these two compositions demonstrated to be printable with a remarkable quality, avoiding common issues of warping and delamination often experienced with the neat PEEK. Particularly, the CF-PEEK/PEI 80/20 formulation showed a very good inter-filament adhesion and with low surface roughness. The CF-PEEK/PEI 40/60 exhibited the highest increase of the T_g (37°C), but the lowest modulus. Future work is required to further investigate thermomechanical properties (e.g., tensile properties at higher temperatures) of the different formulations as well as to evaluate mechanical

properties with optimized printing conditions and 3D printing of samples with different printing configurations. The blends developed in this study could be interesting materials for manufacturing of parts where high service temperature, high mechanical performance or both are of importance.

Acknowledgements

This research was part of a large-collaborative project between Polytechnique Montréal and Safran S.A. (France) through Safran's industrial research Chair on Additive Manufacturing of Organic Matrix Composites (FACMO). The authors acknowledge the financial support from the Natural Sciences and Engineering Research Council of Canada (NSERC) through grant No. CRDPJ 514761-1. The authors also wish to acknowledge financial support of Safran S.A. and would like to thank their industrial affiliates at Safran Composites for their in-kind contributions. The authors would also like to thank Dr. Mihaela Mihai and her team from the National Research Council Canada (Boucherville, QC) for their supports in manufacturing of spooled filaments and Ms. Marie-Hélène Bernier for her assistance with the μ-CT scans.

5. REFERENCES

[1] N. Shahrubudin, T.C. Lee, R. Ramlan, An Overview on 3D Printing Technology: Technological, Materials, and Applications, Procedia Manufacturing. 35 (2019) 1286–1296. https://doi.org/10.1016/j.promfg.2019.06.089.

[2] P. Parandoush, D. Lin, A review on additive manufacturing of polymer-fiber composites, Composite Structures. 182 (2017) 36–53. https://doi.org/10.1016/j.compstruct.2017.08.088.

[3] R.D. Farahani, M. Dubé, D. Therriault, Three-Dimensional Printing of Multifunctional Nanocomposites: Manufacturing Techniques and Applications, Advanced Materials. 28 (2016) 5794–5821. https://doi.org/10.1002/adma.201506215.

[4] D.J. Blundell, B.N. Osborn, The morphology of poly(aryl-ether-ether-ketone), Polymer. 24 (1983) 953–958. https://doi.org/10.1016/0032-3861(83)90144-1.

[5] G.H. Melton, E.N. Peters, R.K. Arisman, 2 - Engineering Thermoplastics, in: M. Kutz (Ed.), Applied Plastics Engineering Handbook, William Andrew Publishing, Oxford, 2011: pp. 7–21. https://doi.org/10.1016/B978-1-4377-3514-7.10002-9.

[6] P.E. Irving, C. Soutis, eds., Polymer Composites in the Aerospace Industry, 1st ed., Elsevier, 2014. https://doi.org/10.1016/C2013-0-16303-9.

[7] P.K. Mallick, Fiber-Reinforced Composites: Materials, Manufacturing, and Design, Third Edition, CRC Press, 2007.
[8] B. Hu, X. Duan, Z. Xing, Z. Xu, C. Du, H. Zhou, R. Chen, B. Shan, Improved design of fused deposition modeling equipment for 3D printing of high-performance PEEK parts, Mechanics of Materials. 137 (2019) 103139. https://doi.org/10.1016/j.mechmat.2019.103139.
[9] W.Z. Wu, P. Geng, J. Zhao, Y. Zhang, D.W. Rosen, H.B. Zhang, Manufacture and thermal deformation analysis of semicrystalline polymer polyether ether ketone by 3D printing, Materials Research Innovations. 18 (2014) S5-12-S5-16. https://doi.org/10.1179/1432891714Z.000000000898.
[10] C. Yang, X. Tian, D. Li, Y. Cao, F. Zhao, C. Shi, Influence of thermal processing conditions in 3D printing on the crystallinity and mechanical properties of PEEK material, Journal of Materials Processing Technology. 248 (2017) 1–7. https://doi.org/10.1016/j.jmatprotec.2017.04.027.
[11] L. Jin, J. Ball, T. Bremner, H.-J. Sue, Crystallization behavior and morphological characterization of poly(ether ether ketone), Polymer. 55 (2014) 5255–5265. https://doi.org/10.1016/j.polymer.2014.08.045.
[12] C. Basgul, T. Yu, D.W. MacDonald, R. Siskey, M. Marcolongo, S.M. Kurtz, Does annealing improve the interlayer adhesion and structural integrity of FFF 3D printed PEEK lumbar spinal cages?, Journal of the Mechanical Behavior of Biomedical Materials. 102 (2020) 103455. https://doi.org/10.1016/j.jmbbm.2019.103455.
[13] J. Hanchi, N.S. Eiss, Dry sliding friction and wear of short carbon-fiber-reinforced polyetheretherketone (PEEK) at elevated temperatures, Wear. 203–204 (1997) 380–386. https://doi.org/10.1016/S0043-1648(96)07347-4.
[14] G.M.K. Ostberg, J.C. Seferis, Annealing effects on the crystallinity of polyetheretherketone (PEEK) and its carbon fiber composite, Journal of Applied Polymer Science. 33 (1987) 29–39. https://doi.org/10.1002/app.1987.070330103.
[15] J. Sandler, P. Werner, M.S.P. Shaffer, V. Demchuk, V. Altstädt, A.H. Windle, Carbon-nanofibre-reinforced poly(ether ether ketone) composites, Composites Part A: Applied Science and Manufacturing. 33 (2002) 1033–1039. https://doi.org/10.1016/S1359-835X(02)00084-2.
[16] M. Yan, X. Tian, G. Peng, D. Li, X. Zhang, High temperature rheological behavior and sintering kinetics of CF/PEEK composites during selective laser sintering, Composites Science and Technology. 165 (2018) 140–147. https://doi.org/10.1016/j.compscitech.2018.06.023.
[17] A. Saleem, L. Frormann, A. Iqbal, High performance thermoplastic composites: Study on the mechanical, thermal, and electrical resistivity properties of carbon fiber-reinforced polyetheretherketone and polyethersulphone, Polymer Composites. 28 (2007) 785–796. https://doi.org/10.1002/pc.20297.
[18] J. Li, L.Q. Zhang, The research on the mechanical and tribological properties of carbon fiber and carbon nanotube-filled PEEK composite, Polymer Composites. 31 (2010) 1315–1320. https://doi.org/10.1002/pc.20916.
[19] S. Berretta, R. Davies, Y.T. Shyng, Y. Wang, O. Ghita, Fused Deposition Modelling of high temperature polymers: Exploring CNT PEEK composites, Polymer Testing. 63 (2017) 251–262. https://doi.org/10.1016/j.polymertesting.2017.08.024.
[20] A.M. Díez-Pascual, M. Naffakh, M.A. Gómez, C. Marco, G. Ellis, J.M. González-Domínguez, A. Ansón, M.T. Martínez, Y. Martínez-Rubi, B. Simard, B. Ashrafi, The influence of a compatibilizer on the thermal and dynamic mechanical properties of PEEK/carbon nanotube composites, Nanotechnology. 20 (2009) 315707. https://doi.org/10.1088/0957-4484/20/31/315707.
[21] S. Kumar, T. Rath, R.N. Mahaling, C.S. Reddy, C.K. Das, K.N. Pandey, R.B. Srivastava, S.B. Yadaw, Study on mechanical, morphological and electrical properties of carbon nanofiber/polyetherimide composites, Materials Science and Engineering: B. 141 (2007) 61–70.
[22] R. Ma, B. Zhu, Q. Zeng, P. Wang, Y. Wang, C. Liu, C. Shen, Melt-Processed Poly(Ether Ether Ketone)/Carbon Nanotubes/Montmorillonite Nanocomposites with Enhanced Mechanical and Thermomechanical Properties, Materials (Basel). 12 (2019). https://doi.org/10.3390/ma12030525.

[23] D.G. Papageorgiou, M. Liu, Z. Li, C. Vallés, R.J. Young, I.A. Kinloch, Hybrid poly(ether ether ketone) composites reinforced with a combination of carbon fibres and graphene nanoplatelets, Composites Science and Technology. 175 (2019) 60–68. https://doi.org/10.1016/j.compscitech.2019.03.006.
[24] J.R. Sarasua, P.M. Remiro, J. Pouyet, The mechanical behaviour of PEEK short fibre composites, Journal of Materials Science. 30 (1995) 3501–3508. https://doi.org/10.1007/BF00349901.
[25] F. Ning, W. Cong, J. Qiu, J. Wei, S. Wang, Additive manufacturing of carbon fiber reinforced thermoplastic composites using fused deposition modeling, Composites Part B: Engineering. 80 (2015) 369–378. https://doi.org/10.1016/j.compositesb.2015.06.013.
[26] M. Mehdikhani, L. Gorbatikh, I. Verpoest, S.V. Lomov, Voids in fiber-reinforced polymer composites: A review on their formation, characteristics, and effects on mechanical performance, Journal of Composite Materials. (2018) 0021998318772152. https://doi.org/10.1177/0021998318772152.
[27] A. Arzak, J.I. Eguiazábal, J. Nazábal, Mechanical performance of directly injection-molded PEEK/PEI blends at room and high temperature, Journal of Macromolecular Science, Part B. 36 (1997) 233–246. https://doi.org/10.1080/00222349708220428.
[28] R. Ramani, S. Alam, Composition optimization of PEEK/PEI blend using model-free kinetics analysis, Thermochimica Acta. 511 (2010) 179–188. https://doi.org/10.1016/j.tca.2010.08.012.
[29] M.J. Jenkins, Crystallisation in miscible blends of PEEK and PEI, Polymer. 42 (2001) 1981–1986. https://doi.org/10.1016/S0032-3861(00)00438-9.
[30] J.E. Harris, L.M. Robeson, Miscible blends of poly(aryl ether ketone)s and polyetherimides, Journal of Applied Polymer Science. 35 (1988) 1877–1891. https://doi.org/10.1002/app.1988.070350713.
[31] M. Shibata, Z. Fang, R. Yosomiya, Miscibility and crystallization behavior of poly(ether ether ketone ketone)/poly(ether imide) blends, Journal of Applied Polymer Science. 80 (2001) 769–775. https://doi.org/10.1002/1097-4628(20010502)80:5<769::AID-APP1153>3.0.CO;2-B.
[32] A.A. Goodwin, G.P. Simon, Glass transition behaviour of poly(ether ether ketone)/poly(ether imide) blends, Polymer. 37 (1996) 991–995. https://doi.org/10.1016/0032-3861(96)87282-X.
[33] Y.S. Chun, H.S. Lee, H.C. Jung, W.N. Kim, Thermal properties of melt-blended poly(ether ether ketone) and poly(ether imide), Journal of Applied Polymer Science. 72 (1999) 733–739. https://doi.org/10.1002/(SICI)1097-4628(19990509)72:6<733::AID-APP1>3.0.CO;2-Y.
[34] L. Lin, N. Ecke, M. Huang, X.-Q. Pei, A.K. Schlarb, Impact of nanosilica on the friction and wear of a PEEK/CF composite coating manufactured by fused deposition modeling (FDM), Composites Part B: Engineering. 177 (2019) 107428. https://doi.org/10.1016/j.compositesb.2019.107428.
[35] X. Han, D. Yang, C. Yang, S. Spintzyk, L. Scheideler, P. Li, D. Li, J. Geis-Gerstorfer, F. Rupp, Carbon Fiber Reinforced PEEK Composites Based on 3D-Printing Technology for Orthopedic and Dental Applications, J Clin Med. 8 (2019). https://doi.org/10.3390/jcm8020240.
[36] A.A. Stepashkin, D.I. Chukov, F.S. Senatov, A.I. Salimon, A.M. Korsunsky, S.D. Kaloshkin, 3D-printed PEEK-carbon fiber (CF) composites: Structure and thermal properties, Composites Science and Technology. 164 (2018) 319–326. https://doi.org/10.1016/j.compscitech.2018.05.032.
[37] S. Ding, B. Zou, P. Wang, H. Ding, Effects of nozzle temperature and building orientation on mechanical properties and microstructure of PEEK and PEI printed by 3D-FDM, Polymer Testing. 78 (2019) 105948. https://doi.org/10.1016/j.polymertesting.2019.105948.
[38] R.J. Zaldivar, D.B. Witkin, T. McLouth, D.N. Patel, K. Schmitt, J.P. Nokes, Influence of processing and orientation print effects on the mechanical and thermal behavior of 3D-Printed ULTEM® 9085 Material, Additive Manufacturing. 13 (2017) 71–80. https://doi.org/10.1016/j.addma.2016.11.007.
[39] ZOLTEK PX35 commercial carbon fiber, https://zoltek.com/wp-content/uploads/2019/01/2021-PX35-Brochure.pdf, Accessed on March 3, 2022.
[40] L.C. Thomas, Modulated DSC® Paper #3 Modulated DSC® Basics; Optimization of MDSC® Experimental Conditions, (2005).
[41] ASTM D3822 / D3822M-14, Standard Test Method for Tensile Properties of Single Textile Fibers, ASTM International, West Conshohocken, PA, 2014. https://doi.org/10.1520/D3822_D3822M-14.

[42] B.S. Hsiao, B.B. Sauer, Glass transition, crystallization, and morphology relationships in miscible poly(aryl ether ketones) and poly(ether imide) blends, Journal of Polymer Science Part B: Polymer Physics. 31 (1993) 901–915. https://doi.org/10.1002/polb.1993.090310801.
[43] S.D. Hudson, D.D. Davis, A.J. Lovinger, Semicrystalline morphology of poly(aryl ether ether ketone)/poly(ether imide) blends, Macromolecules. 25 (1992) 1759–1765. https://doi.org/10.1021/ma00032a021.
[44] G. Crevecoeur, G. Groeninckx, Binary blends of poly(ether ether ketone) and poly(ether imide): miscibility, crystallization behavior and semicrystalline morphology, Macromolecules. 24 (1991) 1190–1195. https://doi.org/10.1021/ma00005a034.
[45] T.G. Fox, Influence of Diluent and of Copolymer Composition on the Glass Temperature of a Polymer System, 1 (1956) 123.
[46] Heon Sang Lee, Woo Nyon Kim, Glass transition temperatures and rigid amorphous fraction of poly(ether ether ketone) and poly(ether imide) blends, Polymer. 38 (1997) 2657–2663. https://doi.org/10.1016/S0032-3861(97)85599-1.
[47] K.M. Rahman, T. Letcher, R. Reese, Mechanical Properties of Additively Manufactured PEEK Components Using Fused Filament Fabrication, (2015) V02AT02A009. https://doi.org/10.1115/IMECE2015-52209.
[48] L.G. Blok, M.L. Longana, H. Yu, B.K. Woods, An investigation into 3D printing of fibre reinforced thermoplastic composites, Additive Manufacturing, (2018) 22, pp.176-186. https://doi.org/10.1016/j.addma.2018.04.039.
[49] N. van de Werken, H. Tekinalp, P. Khanbolouki, S. Ozcan, A. Williams, M. Tehrani, Additively manufactured carbon fiber-reinforced composites: State of the art and perspective, Additive Manufacturing. 31 (2020) 100962. https://doi.org/10.1016/j.addma.2019.100962.
[50] M.M. Porter, N. Ravikumar, F. Barthelat, R. Martini, 3D-printing and mechanics of bio-inspired articulated and multi-material structures, Journal of the Mechanical Behavior of Biomedical Materials. 73 (2017) 114–126. https://doi.org/10.1016/j.jmbbm.2016.12.016.

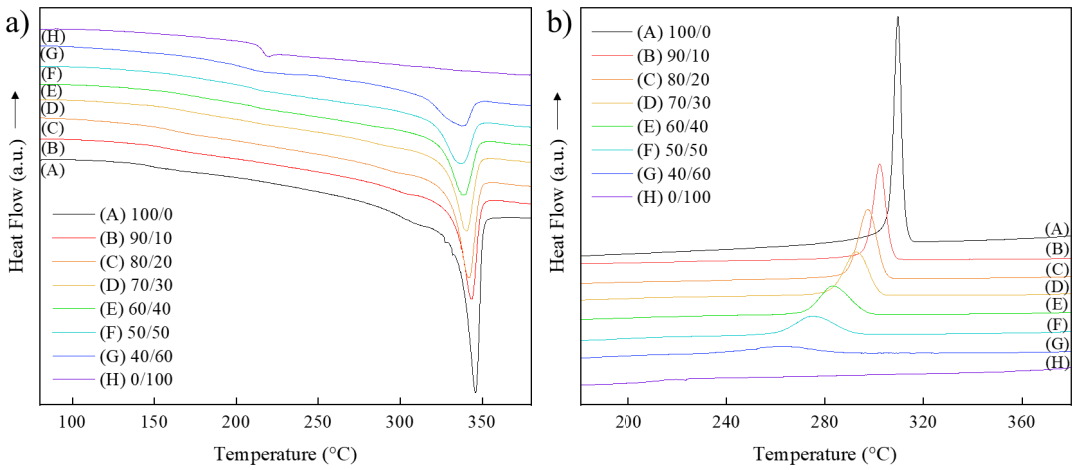

Fig. 1. DSC curves of CF-PEEK/PEI blends at different compositions at a) the second heat run and b) cooling run, recorded from 50°C to 390°C at a rate of 10°C/min. A single peak for the melting and crystalline temperature transitions for all the CF-PEEK/PEI formulations is related to the semi-crystalline behavior of PEEK while their shifting as a function of PEEK/PEI content can be attributable to the miscibility of PEEK and PEI.

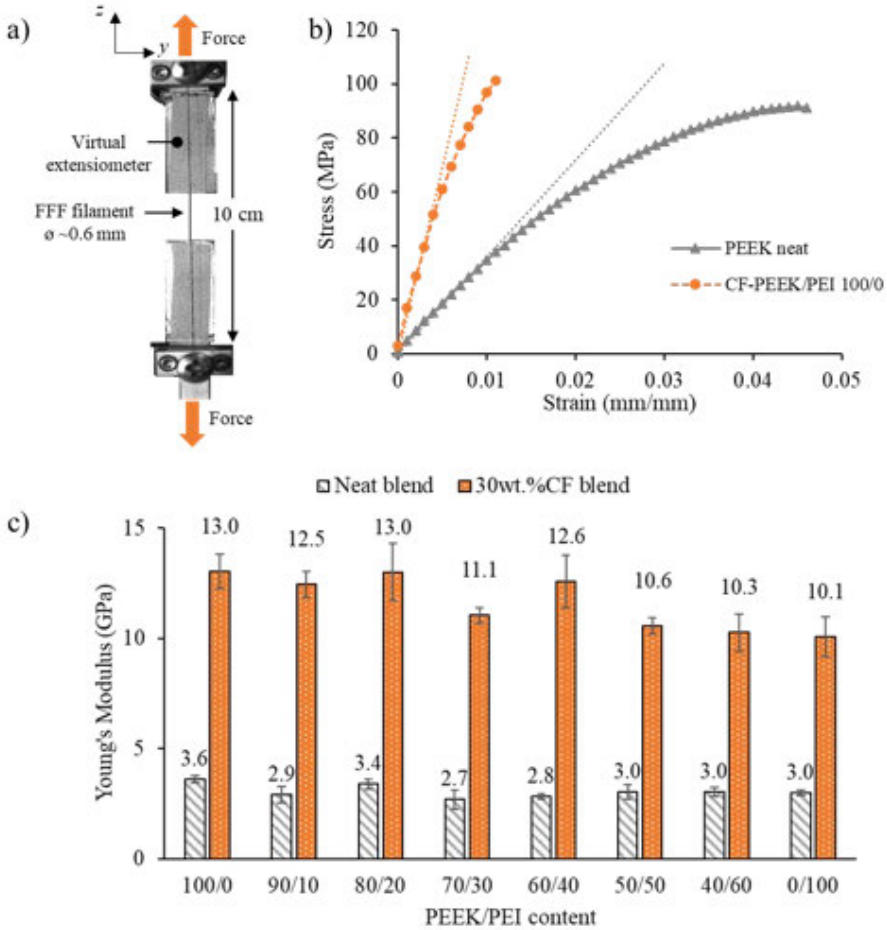

Fig. 2. Tensile mechanical properties of the filaments of the various formulations: a) Photo of the tensile test experimental setup for FFF Filament using a virtual extensometer placed behind the sample, b) Representative stress-strain curves of the PEEK neat and 30wt.%CF-PEEK/PEI 100/0 blend (dotted lines show the elastic regime where modulus is estimated), and c) Young's modulus as a function of the PEEK/PEI blends composition for neat and 30wt.%CF-PEEK/PEI blends FFF filament specimen.

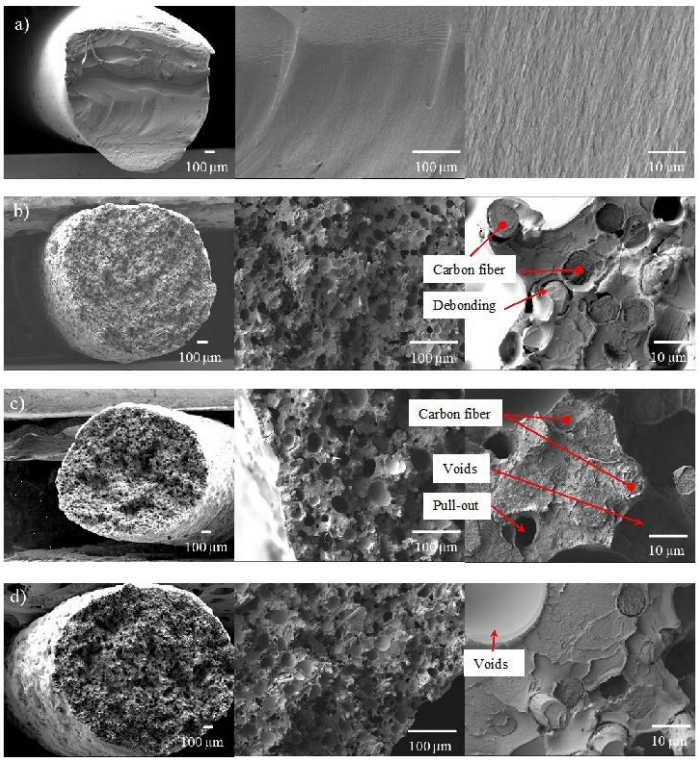

Fig. 3. SEM images at the magnification ×50, ×250, ×2000, of the fractured surface of the extruded filament a) Neat PEEK, b) 30wt.%CF-PEEK/PEI 100/0, c) 30wt.%CF-PEEK/PEI 80/20, and d) 30wt.%CF-PEEK/PEI 50/50. A good distribution of CFs throughout the extruded filament and adhesion between the CF and PEEK/PEI are observed for all the reinforced compositions.

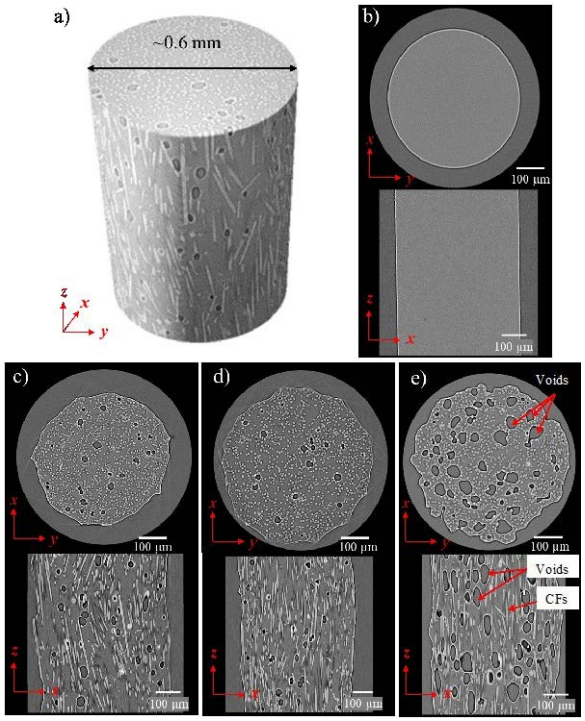

Fig. 4. µ-CT observation of the filaments: a) 3D reconstruction of the µ-CT images of CF-PEEK/PEI 80/20 blend using dragonfly software. µ-CT images of CF-PEEK/PEI blends with the regard of *xy* and *xz* axis for b) Neat PEEK, c) CF-PEEK/PEI 100/0, d) CF-PEEK/PEI 80/20 and e) CF-PEEK/PEI 50/50. The addition of CFs is likely responsible for the creation of voids in the reinforced blends and the void content is higher with increasing PEI proportion.

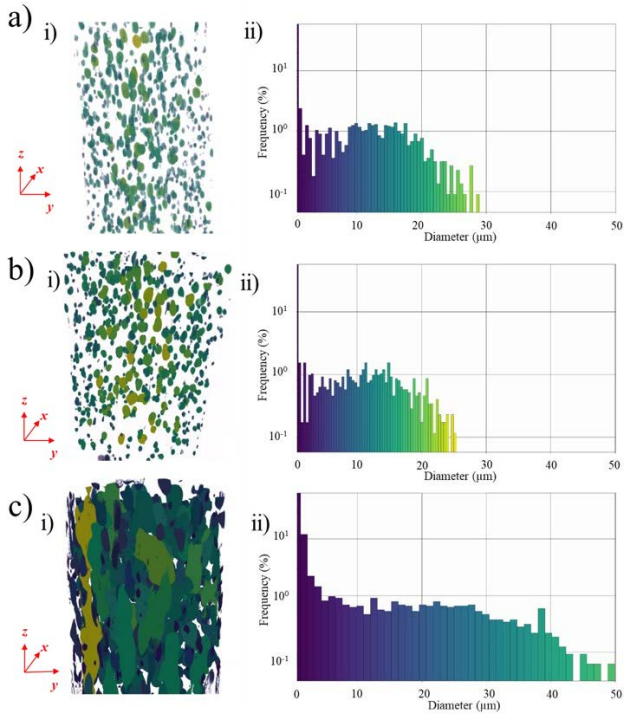

Fig. 5. µ-CT analysis of the voids size distribution a) CF-PEEK/PEI 100/0, b) CF-PEEK/PEI 80/20 and c) CF-PEEK/PEI 50/50, including (i) the 3D visualization of the voids and (ii) the size distribution according to the void's diameter in µm, computed by image segmentation using dragonfly software. The analysis reveals that the degree of porosity of the CF-PEEK/PEI 100/0, CF-PEEK/PEI 80/20 and CF-PEEK/PEI 50/50 is determined at ~3.90%, ~2.40% and ~19.70%, respectively.

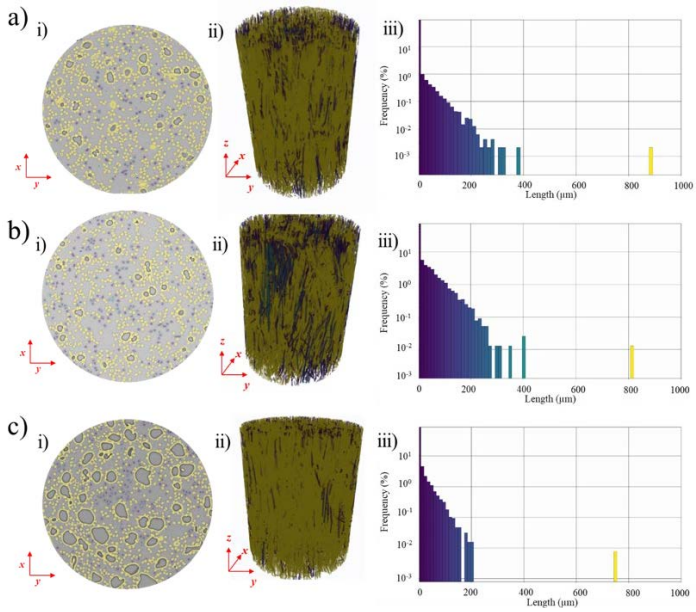

Fig. 6. µ-CT analysis of the CFs length distribution a) CF-PEEK/PEI 100/0, b) CF-PEEK/PEI 80/20 and c) CF-PEEK/PEI 50/50, including (i) the 2D and (ii) 3D visualization of the CFs and (iii) the size distribution according to the CFs length in µm, computed by image segmentation using dragonfly software. The maximum measured CF length is represented by the yellow bar which is associated to the yellow dots in (i). The analysis suggests that the carbon fibers are mostly oriented along the direction of extrusion through the 3D printing nozzle and the majority of CFs length (in yellow) varies between 750 µm to 890 µm.

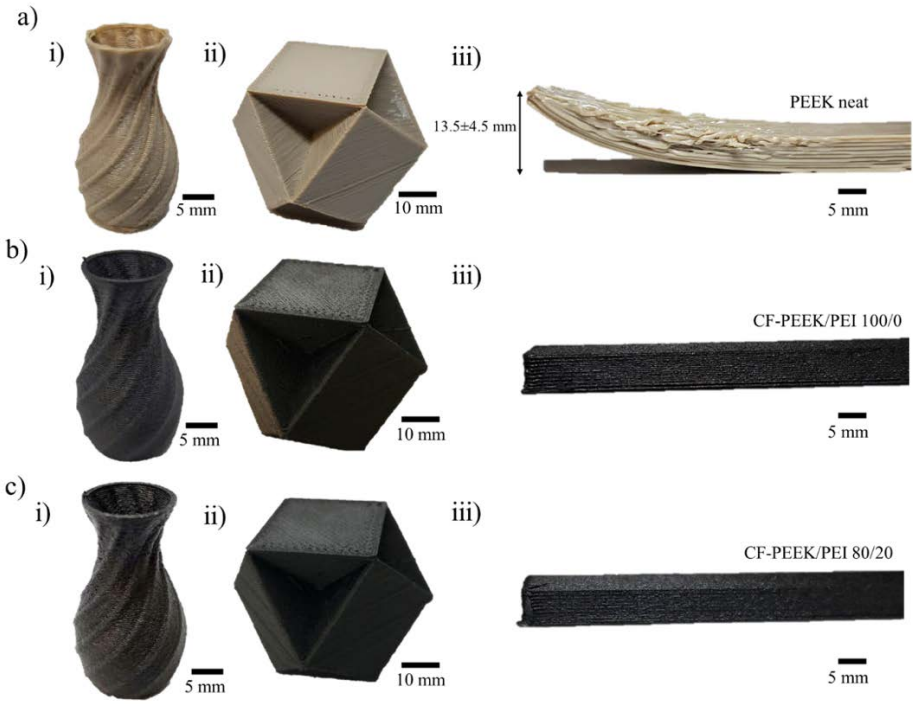

Fig. 7. Optical images of a) neat PEEK, b) 30wt.%CF-PEEK/PEI 100/0 and c) 30wt.%CF-PEEK/PEI 80/20 that have been 3D printed in (i) a vase, (ii) a cubohemioctahedron, and (iii) a rectangular specimen with the dimension 10 cm × 0.8 cm × 0.4 cm to evaluate the FFF 3D printing. The addition of CFs into the blends enabled eliminating the warping issue observed for the neat PEEK.

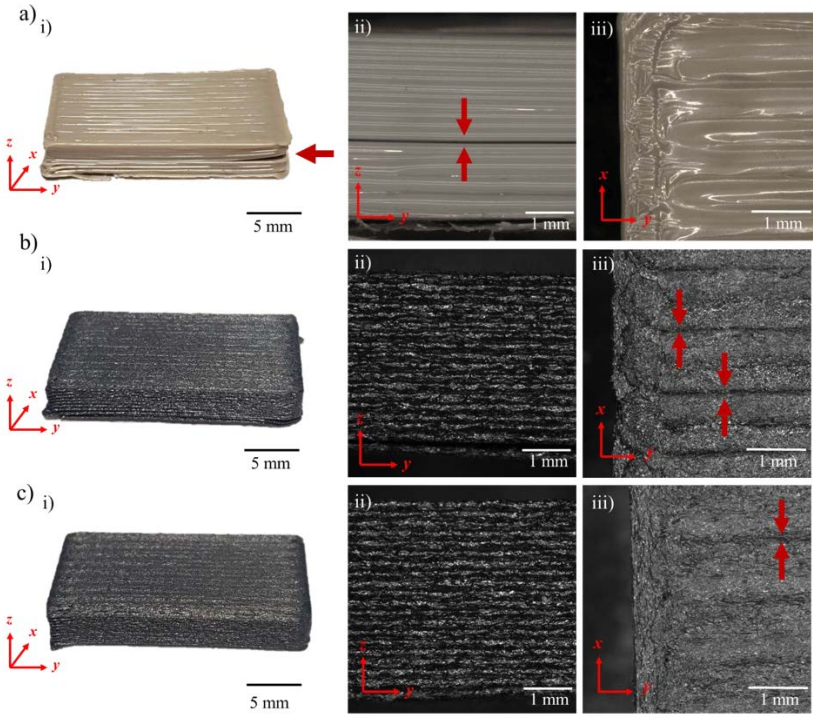

Fig. 8. Comparison of the 3D printed quality of rectangular structures made with a) PEEK neat, b) CF-PEEK/PEI 100/0 and c) CF-PEEK/PEI 80/20; i) Macroscopic pictures of the 3D printed rectangular cuboid specimens 20 mm ×10 mm ×4 mm; ii) Optical microscopic images of the *zy* face highlighting the layer-by-layer deposition; iii) Optical microscopic images of the top length surface *xy* highlighting the inter-filament bonding. The red arrows indicate the position of gaps present in the 3D printed structure. The inter-filament adhesion improved for the reinforced blends.

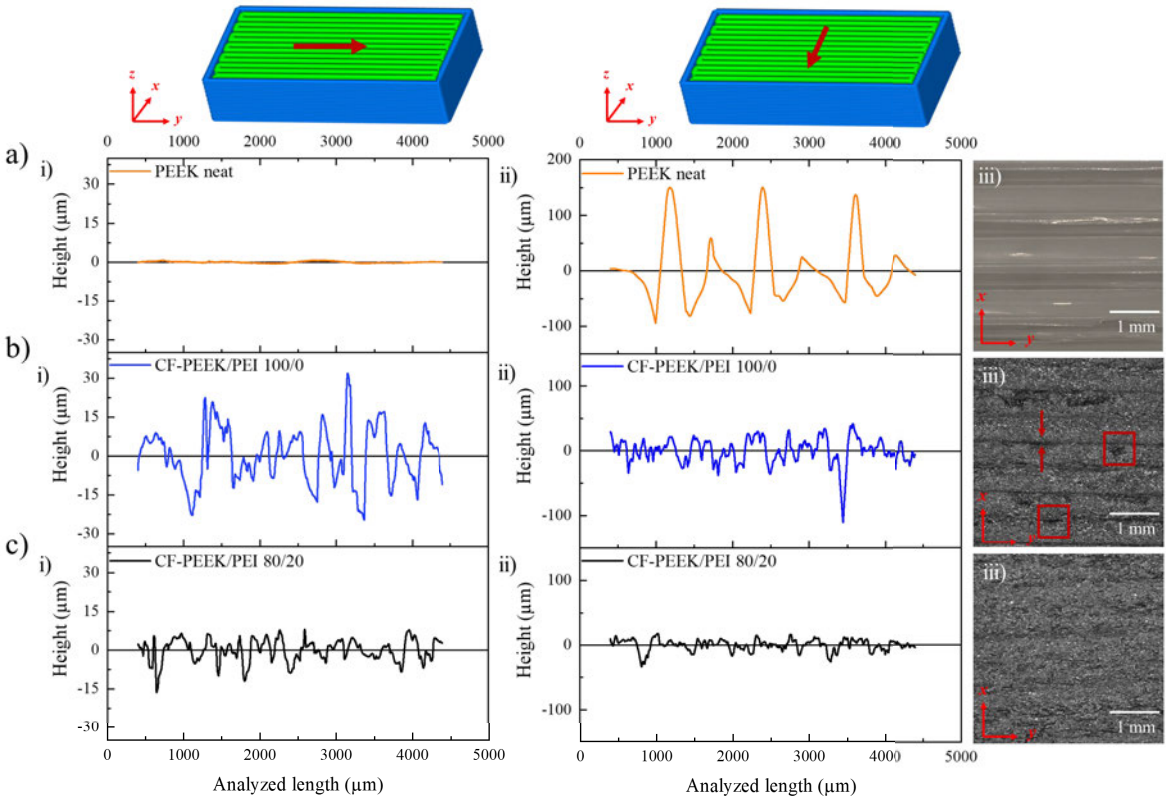

Fig. 9. Surface roughness profile comparison of the 3D printed rectangular cuboid's top surface, made of a) PEEK neat, b) CF-PEEK/PEI 100/0 and c) CF-PEEK/PEI 80/20, (i) in the lengthwise direction and (ii) the crosswise direction. The infill pattern used are shown in green, and the outline perimeter in blue. (iii) Microscopic images of the analyzed surface for roughness test for PEEK neat, CF-PEEK/PEI 100/0 and CF-PEEK/PEI 80/20. The printing defects are highlighted using red arrows and red squares.

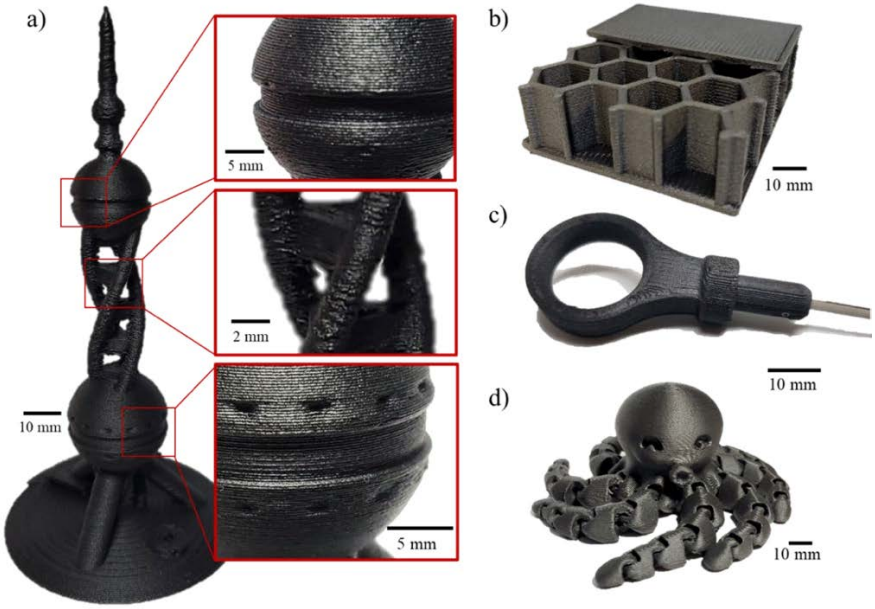

Fig. 10. Optical images of 3D printed demonstrators made of CF-PEEK/PEI 80/20 blend a) 3D representation of the Oriental Pearl Tower of Shanghai used as 3D printer torture test, b) a honeycomb sandwich panel structure c) a ring for the oil ruler, d) an articulated octopus structure. The high quality of the complex structures further proves the printability and viability of CF-PEEK/PEI 80/20.

Table 1. DSC results for 30wt.%CF-PEEK/PEI blends reporting T_c from the cooling run, T_m, X_c% *and* ΔH_m from the second heating run.

PEEK/PEI weight ratio (as 70 wt.% matrix)	T_c (°C)	T_m (°C)	X_c (%)	ΔH_m (J/g)
100/0	307.8	344.8	31.9	29.0
90/10	302.2	343.2	35.1	28.8
80/20	297.6	341.6	40.5	29.5
70/30	292.6	340.2	37.7	24.0
60/40	283.2	337.5	38.1	20.8
50/50	274.8	336.1	41.0	18.7
40/60	262.3	337.1	40.1	14.6
0/100	-	-	-	-

Table 2. mDSC measurements of the T_g for 30wt.%CF-PEEK/PEI blends and their comparison to calculated *Fox* T_g. Some blends exhibited a second T_g.

PEEK/PEI weight ratio (as 70 wt.% matrix)	T_{gFox} (°C)	T_g (°C)	2nd T_g (°C)
100/0	143.0	143.0	-
90/10	148.0	147.0	-
80/20	153.5	153.8	-
70/30	159.3	162.3	217.7
60/40	165.6	167.8	213.0
50/50	172.4	176.5	210.4
40/60	179.8	178.4	207.3
0/100	217.0	217.6	-

Table 3. FFF parameters of the 3D printed structures.

3D printed structures	Printing parameters and 3D printed part	PEEK neat CF-PEEK/PEI 100/0	CF-PEEK/PEI 80/20
All structures	Nozzle diameter (mm)	0.6	0.6
	Nozzle temperature (°C)	400	380
	Bed temperature (°C)	180	150
	Chamber temperature (°C)	120	120
	Layer height (mm)	0.2	0.2
Vase	Infill (%)	0	0
	Speed (mm/s)	50	50
Cubohemioctahedron	Infill (%)	30	30
	Speed (mm/s)	40	40

Rectangular cuboid (100 × 8 × 4) mm^3 (20 × 10 × 4) mm^3	Infill (%)	100	100
	Speed (mm/s)	30	30

Table 4. Arithmetical mean roughness parameter *Ra* for PEEK neat, CF-PEEK/PEI 100/0 and CF-PEEK/PEI 80/20 material, according to the lengthwise direction and the crosswise direction measured on the top layer.

Material	*Ra* (µm) Lengthwise direction	*Ra* (µm) Crosswise direction
PEEK neat	0.2	37.9
CF-PEEK/PEI 100/0	8.5	14.6
CF-PEEK/PEI 80/20	3.2	6.6

Table 5. Printing parameters of the 3D printed part presented in Fig. 10.

Part in Fig. 10	Main parameters	Infill (%)	Speed (mm/s)
Tower	Nozzle diameter: 0.6 mm Nozzle temperature: 380°C Bed temperature: 150°C Chamber temperature: 120°C Layer height: 0.2 mm	30	30
Sandwich panel		100	40
Ring		100	40
Articulated octopus		100	30

Video 1. 3D visualization of the segmentation and identification of the voids (purple), CF (dark blue) and the PEEK/PEI matrix (grey), for the CF-PEEK/PEI 80/20 blend. The scanned sample is an FFF filament with a diameter of 0.6 mm, extruded through a nozzle at 400°C with a speed of 5 mm/s.